5 Isotope effects on vibrational relaxation and hydrogen-bond dynamics in water

Pump–probe experiments HDO dissolved in liquid H_2O show the spectral dynamics and the vibrational relaxation of the OD stretch vibration. We find a correlation time $\tau_c = 0.40$ ps for the spectral diffusion and a lifetime $T_1 = 1.8$ ps for the vibrational relaxation. These values differ significantly from those of the OH stretch vibration of HDO:D_2O.

5.1 Introduction

Most time-resolved experiments on water in this thesis and in the literature[33,129,135,132] are devoted to isotopically diluted aqueous systems, i.e. HDO in D_2O instead of H_2O. This is to avoid strong heating effects and to be able to study the behavior of an 'isolated' OH group (§1.1, §1.2, §2.8). The OD stretch vibration in D_2O has a frequency of $\approx$2500 cm^{-1}, compared to $\sim$3400 cm^{-1} for the OH stretch vibration in H_2O. Thus, resonant energy-transfer from an excited OH group to an OD group is not possible.

However, though chemically very similar, H_2O and D_2O are not identical. Because the mass of the D atom is twice as large as the H atom, many processes that involve hydrogen bonds or the transfer of a proton have different kinetics if the proton is replaced by a deuteron. One consequence of this difference is that animals, including humans, cannot live if more than 20% of the water in their body is replaced by heavy water.[64] In the previous chapter, we saw that the vibrational lifetime of the OH stretch vibration of HDO in D_2O is $T_1 = 740$ fs. Further, the frequency of an individual OH group is known to vary in time with a time constant of $\approx$600 fs.[33,129] (Chapter 8 will discuss this in more detail). This so-called spectral diffusion is the direct result of hydrogen-bond length fluctuations, i.e. the O–O distance R in the DO$-$H$\cdots$OD_2. Though the OH group contains a proton, for R to vary, the hydrogen-bond accepting D_2O molecule must move, which necessarily changes the surrounding 'deuteron-bond' structure. Therefore, the timescale of spectral diffusion in HDO:D_2O is likely to be more representative of the deuteron-bond dynamics of the solvent, D_2O, than of the hydrogen-bond dynamics in ordinary water.

Time-resolved experiments on the OH stretch vibration in pure H_2O have been done, but it is difficult to extract information on the hydrogen-bond dynamics due to rapid resonant energy transfer between the OH groups[21,131] and the overwhelmingly strong thermal effects.[74] However, in the same way that the experiments on the OH stretch vibration of HDO in D_2O provide information on the deuteron-bond dynamics of the solvent, an experiment on the OD stretch vibration of HDO in H_2O will yield information on the hydrogen-bond dynamics of ordinary water.

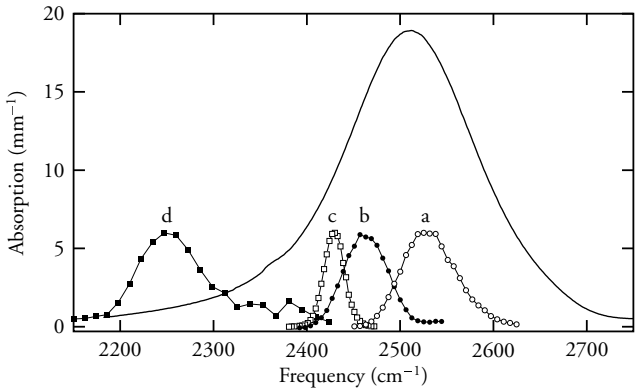

FIGURE 5.1. Absorption band of the OD stretch vibration in HDO:H_2O (solid line), corrected for the H_2O background. The data points indicate the spectra of the probe pulses, the letters a–d correspond to those in Fig. 5.2.

5.2 EXPERIMENT

The experiments were pump–probe measurements where a femtosecond infrared laser pulse excited the $v = 0 \rightarrow 1$ transition of the OD stretch vibration of HDO molecules dissolved in H_2O. The frequency of this transition is approximately 2500 cm^{-1}. The transmittance of a subsequent probe pulse with an independently tunable frequency is a measure of the degree of excitation of the OD groups in the solution.

The general background on pump–probe experiments is discussed in §1.2; the details of the pulse generation in §2.2.5; and the pump–probe setup in §2.4.1. The sample was a 50-μm-thick layer of about 5% HDO in H_2O. Sample thickness and concentration were chosen such that the transmittance at the center of the OD absorption band was approximately 5%. The concentration is necessarily relatively high, compared to the concentration in the HDO:D_2O experiments in this thesis, because pure H_2O contributes significantly to the absorbance around 2500 cm^{-1}. The high HDO concentration ensures that most of the pump energy is actually used to excite the OD vibration. During the measurements, the sample was continuously rotated to avoid heating effects due to previous pulses (see also §2.8). The experiments were conducted at room temperature (298 K).

Basically, each measurement yields a transient absorbance change $\Delta\alpha(t)$ that changes with the time t after excitation of the OD stretch vibration by the pump pulse. Between measurements, we varied the pump frequency and/or probe frequency.

5.3 RESULTS

The absorption band of the OD stretch vibration is centered at 2500 cm^{-1} and has an FWHM of 170 cm^{-1} (see Fig. 5.1). Figure 5.2 shows the time dependence of the absorbance change $\Delta\alpha(t)$ for different pump and probe frequencies. Clearly, the pump–probe signal depends strongly on the employed frequencies.

At delays shorter than 1 ps, the signals display very complex behavior: in Figs. 5.2a

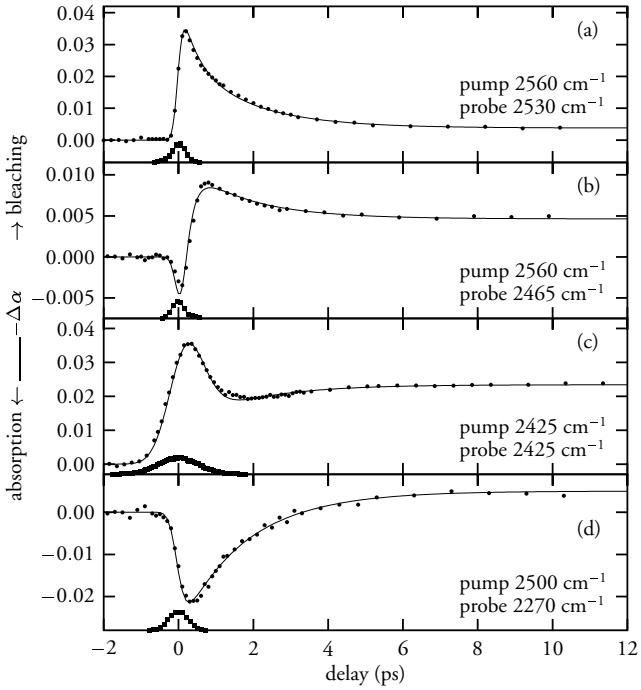

FIGURE 5.2. Measured pump-probe transients of HDO:H_2O at different pump and probe frequencies. The solid line is a fit to the data [Eq. (5.14)]. Also shown are cross-correlation traces of the pump and probe pulses.

and 5.2c, a bleaching signal is observed; Fig. 5.2d shows an induced absorption due to the $1 \rightarrow 2$ transition. In Fig. 5.2b, within 1 ps, the initial absorbance changes into a bleaching signal. The initial behavior, within $\sim$1 ps after excitation, depends strongly on both pump and probe frequencies. For instance, the initial absorption at a 2465 cm^{-1} probe frequency (Fig. 5.2b) is not visible with a pump frequency of 2465 or 2500 cm^{-1} (not shown), instead of 2560 cm^{-1}. The bleaching at 2425 cm^{-1} (Fig. 5.2c) is not visible with a pump frequency of 2560 cm^{-1}; an induced absorption appears instead. The fact that the initial behavior depends on both pump and probe frequencies, suggests that spectral diffusion significantly affects the signals at $t < 1$ ps.

More than $\sim$1 ps after excitation, all signals either increase (Figs. 5.2c and 5.2d) or decrease (Figs. 5.2a and 5.2b) exponentially to a nonzero level, all with the same time constant of 1.8 ps. The persistent absorbance change at large delays is due to the temperature increase that results from the thermalisation of the pump pulse energy. Raising the temperature causes the absorption band to shift to the blue and become weaker.[31] At most frequencies, a temperature increase leads to a decrease in absorption, except at the frequencies far in the high-frequency wing of the absorption band, where the absorption increases. The facts that, for $t > 1$ ps, all signals have an equal decay time and their signs are independent of the pump frequency, indicate that the distribution of excited OD groups over the spectrum is equilibrated due to spectral diffusion. The decay time of 1.8 ps

is therefore equal to the vibrational lifetime T_1.

5.4 The Brownian-oscillator model

To describe the pump–probe signals on a distribution of OD groups that is subject to spectral modulation, we use a modified[129] Brownian-oscillator[88] model. The Brownian-oscillator model describes the frequency modulation of an ensemble of OD groups, each of which has a certain bandwidth around a central frequency ω_B for its $v = 0 \rightarrow 1$ transition. The idea behind this model is that spectral diffusion of the frequency of a particle corresponds to diffusion in a harmonic potential, or 'Brownian oscillation' (analogous to 'Brownian motion') of a low-frequency coordinate. In this case, the low-frequency coordinate is the 'hydrogen' bond length R, i.e. the O–D···O length. In more isolated hydrogen-bonded systems, such an oscillation can take place.[78] The present model is a Brownian oscillator in the overdamped limit, which excludes oscillations in R. In thermal equilibrium, the population of the $v = 0$ state corresponds to an absorption spectrum

$$f_d(\omega) \propto \exp\left(-(\omega - \omega_B)/2\Delta_d^2\right), \tag{5.1}$$

where Δ_d defines the diffusive bandwidth. The fact that the excitation frequency of the OD group depends on R implies that the excited-state potential $W_1(R)$ has its minimum at a value of R that differs from that of the minimum of the ground-state potential $W_0(R)$ (see Fig. 5.3). In a pump–probe experiment, the bleaching of the $v = 0 \rightarrow 1$ transition depends on both the populations of the $v = 0$ and the $v = 1$ states. This means that, if the excited-state population is equilibrated within the $v = 1$ potential, the $v = 1 \rightarrow 0$ contribution to the bleaching is centered at a frequency $\omega_B - \delta\omega_{sto}$, where $\delta\omega_{sto}$ is the Stokes shift. This Stokes shift and the diffusive bandwidth Δ_d have the relation

$$\delta\omega_{sto} = \hbar\Delta_d^2/k_B T, \tag{5.2}$$

where $\hbar$ is Planck's constant divided by 2π and k_B is Boltzmann's constant. If we assume that the modulation of the spectral frequency is a diffusive process, the correlation time τ_c is defined by the statistical behavior of the frequency $\omega(t)$ of an individual OD group:

$$\langle(\omega(t) - \omega_B)(\omega(0) - \omega_B)\rangle = \Delta_d^2 e^{-t/\tau_c}. \tag{5.3}$$

The absorbance change in a pump–probe experiment has three contributions: ground-state depletion, stimulated emission from the excited-state population, and excited-state absorption. These three contributions correspond to the $v = 0 \rightarrow 1$, the $v = 1 \rightarrow 0$, and the $v = 1 \rightarrow 2$ transitions, respectively. We assume that the pump and probe pulses have Gaussian shapes with central frequencies ω_{pu} and ω_{pr}, and RMS bandwidths Δ_{pu} and Δ_{pr}, e.g. $\exp([\omega - \omega_{pu}]^2/2\Delta_{pu}^2)$. The spectral dynamics of the bleaching signal at delay t, with pump frequency ω_{pu} and probe frequency ω_{pr}, are described by

$$B(\omega_{pu}, \omega_{pr}, t) = A\left[B_{01}(t) + B_{10}(t) - \sigma B_{12}(t)\right] \quad (t > 0). \tag{5.4}$$

where ω_{pu} and ω_{pr} are the pump and probe frequency, respectively; A is the amplitude of the signal that depends on how efficiently the pump pulse excites the Brownian oscillator

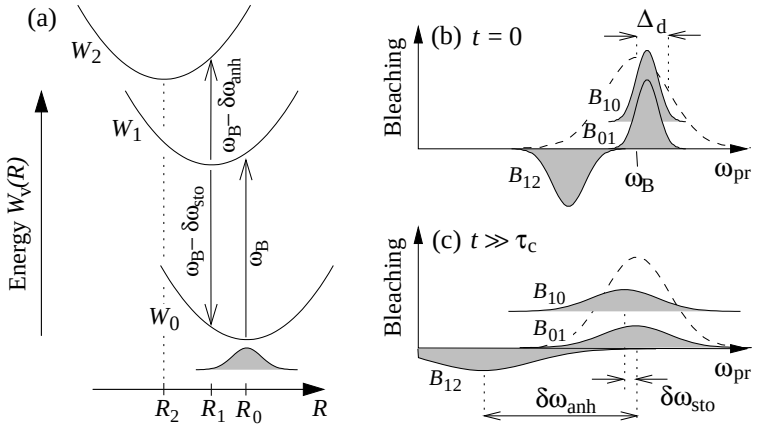

FIGURE 5.3. In (a), schematic potentials of the Brownian oscillator model. The potential energy is a parabolic function of the hydrogen bond length R for every state v of the OH stretch vibration. The central frequency for a thermal population (shaded area) in the ground-state potential is ω_B. For a thermal population at the bottom of the $v = 1$ potential, the $v = 1 \to 0$ transition frequency has a Stokes shift $\delta\omega_{sto}$ and the $v = 1 \to 2$ transition frequency has an anharmonic red-shift $\delta\omega_{anh}$. The relative position of the $v = 2$ potential is defined by $a = (R_2 - R_1)/(R_1 - R_0)$. In (b) and (c), the contributions B_{ij} to the transient spectrum [Eq. (5.4)] are shown schematically, for a pump frequency slightly larger than ω_B. The dashed line indicates the linear absorption spectrum.

ensemble. The terms B_{ij} represent the contributions to the probe signal for the $v = i \to j$ transitions. Equation (5.4) does not yet incorporate vibrational relaxation. If we assume that pump and probe pulses have Gaussian spectra with standard deviations Δ_{pu} and Δ_{pr}, respectively, the components in Eq. (5.4) are

$$A = \exp\left(-(\omega_{pu} - \omega_B)^2/2(\Delta_d^2 + \Delta_{pu}^2)\right), \tag{5.5}$$

$$B_{01}(t) = D^{-1}(t)\exp\left(-\left[\omega_{pr} - \omega_{01}(t)\right]^2/2D^2(t)\right) \tag{5.6}$$

$$B_{10}(t) = D^{-1}(t)\exp\left(-\left[\omega_{pr} - \omega_{10}(t)\right]^2/2D^2(t)\right) \tag{5.7}$$

$$B_{12}(t) = D^{-1}(t)\exp\left(-\left[\omega_{pr} - \omega_{12}(t)\right]^2/2a^2D^2(t)\right) \tag{5.8}$$

$$D^2(t) = \Delta_d^2\left(1 - \frac{\Delta_d^2}{\Delta_d^2 + \Delta_{pu}^2}e^{-2t/\tau_c}\right) + \Delta_{pr}^2. \tag{5.9}$$

The B_{01} and B_{10} contributions have identical widths $D(t)$, and the B_{12} contribution has a width $aD(t)$, where a is a scaling factor (see Fig. 5.3). The quantity σ is the relative cross-section of the $v = 1 \to 2$ transition as compared to the $v = 0 \to 1$ transition. The time-dependent frequencies $\omega_{ij}(t)$ are

$$\omega_{01}(t) = \omega_B + e^{-t/\tau_c}(\omega_{hl}^0 - \omega_B), \tag{5.10A}$$

$$\omega_{10}(t) = \omega_B - \delta\omega_{sto} + e^{-t/\tau_c}(\omega_{hl}^0 + \delta\omega_{sto} - \omega_B), \tag{5.10B}$$

$$\omega_{12}(t) = \omega_B - \delta\omega_{anh} + ae^{-t/\tau_c}(\omega_{hl}^0 + \delta\omega_{sto} - \omega_B), \tag{5.10C}$$

with the correlation time τ_c, the anharmonic shift $\delta\omega_{anh}$, and the Stokes shift $\delta\omega_{sto}$, and the initial frequency of the bleaching

$$\omega_{hl}^{o} = \frac{\Delta_{pu}^2}{\Delta_{pu}^2 + \Delta_d^2}\omega_B + \frac{\Delta_d^2}{\Delta_{pu}^2 + \Delta_d^2}\omega_{pu}, \tag{5.11}$$

where we assume a sample that is not optically dense. In the present chapter, we corrected for the high optical density, which means that the initial hole distribution is the product of the pump spectrum $f_{pu}(\omega)$ and the absorption spectrum $1 - T_o(\omega)$. The effect of this correction on the resulting hole is rather small, though. The width $D(t = 0)$ and the frequency ω_{hl}^{o} define the Gaussian shape of spectral hole directly after excitation. This Gaussian shaped hole is the product of the excitation spectrum and the population distribution, which are both assumed Gaussian as well. Equation (5.4) does not yet incorporate vibrational relaxation, which we include as an exponentially decaying factor in the expression

$$\Delta\alpha_B(\omega_{pu}, \omega_{pr}, t) = -e^{-t/T_1}B(\omega_{pu}, \omega_{pr}, t) \quad (t > 0) \tag{5.12}$$

for the absorbance change.

5.5 Thermalization and fits

Equation (5.12) does not yet incorporate the effects of thermalization, i.e. the persistent absorbance change at larger delays that is visible in the experimental data in Fig. 5.2. We assume that thermalization is a separate term in the experimental absorbance change $\Delta\alpha$ that is proportional to the total amount of energy released by vibrational relaxation. Hence, this term reads

$$\Delta\alpha_T(t) = \sigma_T\left(1 - e^{-t/T_1}\right) \quad (t > 0), \tag{5.13}$$

where σ_T is an amplitude that is different for each measurement, because it depends on the probe frequency and the exact amount of absorbed pump pulse energy. Thus, the absorbance change as measured in an experiment is described by the convolution of the pump–probe pulse cross-correlate and the sum of Eqs. (5.12) and (5.13), resulting in

$$\begin{aligned}\Delta\alpha(\omega_{pu}, \omega_{pr}, t) \\ = \int_{-\infty}^{\infty} dt' \left[\Delta\alpha_B(\omega_{pu}, \omega_{pr}, t') + \Delta\alpha_T(t)\right] \exp\left(-\frac{(t - t')^2}{2\tau_p^2}\right),\end{aligned} \tag{5.14}$$

which can be evaluated numerically. The quantity τ_p defines the width of the pump–probe pulse cross-correlate.

All data can be described by Eq. (5.14) with the parameters in Table 5.1, as resulting from a fit. The solid lines in Fig. 5.2 correspond to the fit, which accurately describe all features of the experimental data. For example, pumping at the low-frequency side of the absorption band (2425 cm^{-1}, Fig. 5.2c) affects molecules with a short hydrogen-bond length R that corresponds to the frequency of the pump pulse (see Fig. 5.3). At short delays, the probe pulse, having the same frequency as the pump pulse, experiences a

TABLE 5.1. Fitted model parameters. The rightmost column shows the parameters for the OH stretch vibration of HDO:D_2O from Ref. 129.

Parameter		HDO:H_2O OD stretch	HDO:D_2O OH stretch
Vibrational lifetime	T_1 (ps)	1.8	0.74
Spectral correlation time	τ_c (ps)	0.40	0.5
Central frequency	ω_B (cm^{-1})	2520	3400
Spectral RMS deviation	Δ_d (cm^{-1})	72	101
Anharmonic redshift	$\delta\omega_{anh}$ (cm^{-1})	170	270
Stokes shift	$\delta\omega_{sto}$	24[b]	74
R shift for $v = 2$ potential	a	1.4	2
Relative $v = 1 \rightarrow 2$ cross-section	σ	1.38	1.54

[b] this value is not a fit parameter, but results from Eq. (5.2)

bleaching. However, both the $v = 0$ depletion ('hole') and the $v = 1$ population ('particle') distributions evolve in time, predominantly towards the minima of their potentials. The time evolution of the particle and hole distributions is such that the $v = 0 \rightarrow 1$ bleaching contributions shift out of the frequency window of the probe, while the $v = 1 \rightarrow 2$ absorption moves into the probe window. Both processes result in the rapid increase of $\Delta\alpha$ for $t < 1.5$ ps. At the same time, the thermalization of the vibrational excitation causes a slowly-growing ($T_1 = 1.8$ ps) negative contribution, which is superimposed on the fast initial processes resulting from spectral diffusion.

In Fig. 5.2b, the excitation frequency is at the high-frequency side of the OD absorption band, while the probe frequency is at the low-frequency side. Here, the situation is the reverse of that in Fig. 5.2c: initially, the probe experiences an induced absorption due to the $v = 1 \rightarrow 2$ transition. During the spectral diffusion in the first $\sim$1 ps, this induced absorption contribution shifts out of the probe window, while the bleaching of the $v = 0 \rightarrow 1$ state shifts into the probe window. Again, the thermalization of the excitation causes a slow decay of the bleaching to an equilibrium value corresponding to a higher temperature of the sample.

5.6 DISCUSSION

The observed lifetime $T_1 = 1.8$ ps of the OD stretch vibration of HDO:H_2O is in agreement to the value of approximately 2 ps for the lifetime of the OD stretch vibration in pure D_2O that was measured by time-resolved anti-Stokes Raman experiments.[21] The similarity of these numbers for the pure liquid and the isotopically diluted solution is quite surprising, since for the OH stretch vibration, the lifetime in pure H_2O is much shorter than in the diluted solution: $\sim$200 fs versus 740 fs.[74] The latter difference can be explained from the fact that in pure H_2O, where the distance between adjacent OH groups is small, the energy of an OH oscillator is rapidly transfered to nearby oscillators. This Förster energy transfer[29] causes very fast spectral diffusion, and enables the vibration to find its most efficient relaxation path.[130] Comparison of the OD stretch lifetime in HDO:H_2O

(this chapter) and in pure D_2O (Ref. 21) thus seems to indicate that intermolecular energy transfer plays a much smaller role for the OD stretch vibration than for the OH stretch. The less important role of intermolecular energy transfer in the vibrational relaxation of D_2O can be at least partly explained from the somewhat smaller transition dipole moment of the OD stretch vibration.

The lifetime of the OD stretch vibration is more than twice as long as the lifetime of the OH stretch vibration. This is an interesting observation, since it conflicts with the energy-gap law,[91] which states that the vibrational relaxation time is proportional to δ^{-N}, where $\delta \ll 1$ and N is the number of quanta dissipated in a particular accepting mode. For a lower-frequency vibration (e.g. the OD stretch vibration compared to the OH stretch vibration), N is generally smaller, which would imply a shorter lifetime. In this case, however, the lower-frequency OD vibration lives *longer* than the higher-frequency OH vibration. It should be noted that, in addition to energy gap considerations, there are several other effects that determine the isotope effect in the vibrational lifetime, such as coupling strengths and the density-of-states of combined accepting modes.

In most vibrational relaxation processes, the energy is not transfered to a single accepting mode, but rather to a combination of modes, that may consist of one high-frequency mode that accepts the major part of the energy (e.g. the bending mode, $\sim$1450 cm^{-1}) and several low-frequency modes to compensate for the energy difference, or many low-frequency modes (e.g. the hydrogen-bond stretch mode, $\sim$200 cm^{-1}). For high-frequency vibrations in the condensed phase, there are many combinations of accepting modes that match the energy to be dissipated. The sheer number of combinations may compensate for the larger number N of quanta and can therefore cause the higher relaxation rate of the OH stretch mode compared to the lower-frequency OD stretch mode.

Apparently, the number of accepting modes for the OH stretch mode in $HDO:D_2O$ is larger than those for the OD stretch mode of $HDO:H_2O$ by an amount sufficiently large for the OH stretch lifetime to be shorter than the OD stretch lifetime, despite the larger energy gap.

In zeolites,[10] an OD stretch mode relaxes about three time as fast as an OH mode. From the temperature dependence of the vibrational lifetime, the numbers of quanta of accepting modes were determined to be 5 and 3, respectively. The energy-gap law would predict a much larger difference in lifetime than the observed factor 3. Again, the difference in the number of accepting mode combinations may explain the small difference in vibrational lifetimes.

It is not yet clear which are the accepting modes in the relaxation of an excited OD or OH stretch vibration in water. Two likely accepting modes are the HOD bending vibration, and the hydrogen-bond mode. In Chapter 4, we saw that the temperature and frequency dependence of the OH stretch lifetime for $HDO:D_2O$ can be well explained if the relaxation involves energy transfer to the hydrogen bond. However, the Raman experiments[21] showed that the energy relaxation of both the OH and OD stretch modes leads to a transient excitation of the bending mode. Unfortunately, in the present experiments, we are not able to determine the precise relaxation mechanism. Probably, both the HOD bending mode and the hydrogen-bond mode play a role in the relaxation mechanism.

For the OH stretch vibration of $HDO:D_2O$, pump–probe experiments similar to the ones discussed here yielded values for the spectral diffusion correlation time of 500 fs[129] and

700 fs.[33] (In Chapter 8, we will discuss spectral diffusion in HDO:D_2O in more detail). Since the frequency of the OH vibration is determined by the length of the hydrogen bond that binds the hydrogen atom to the oxygen atom of a nearby water molecule (see §1.1 and Fig. 8.2 on page 90) its dynamics result from the motion of the bulk D_2O molecules. In the present experiment, we studied the OD stretch vibration in a dilute solution of HDO in H_2O. The value $\tau_c = 0.40$ ps for the spectral correlation time is directly related to the motion of H_2O molecules. In measuring this value, the OD excitation serves only as a label to follow these motions. The fact that the vibrational lifetime T_1 is relatively large allows for a very precise determination of τ_c. The difference with HDO:D_2O implies that H_2O molecules show significantly faster hydrogen-bond dynamics than D_2O.

5.7 Conclusions

We performed two-color mid-infrared pump-probe experiments on the OD stretch vibration in HDO:H_2O. The data displayed the effects of spectral diffusion, which were modeled with a Brownian-oscillator model. The vibrational lifetime of the OD stretch vibration is 1.8 ps and its spectral correlation time is 400 fs. The vibrational lifetime of the OD stretch vibration is significantly longer than that of the OH stretch vibration. The spectral diffusion correlation time is shorter than previously obtained for D_2O, which means that the hydrogen-bond dynamics is faster in H_2O than in D_2O.